Hindawi Publishing Corporation
International Journal of Photoenergy
Volume 2014, Article ID 471713, 9 pages
http://dx.doi.org/10.1155/2014/471713

Research Article

Modification of One-Dimensional TiO_2 Nanotubes with CaO Dopants for High CO_2 Adsorption

Chin Wei Lai

Nanotechnology & Catalysis Research Centre (NANOCAT), Institute of Postgraduate Studies (IPS), Universiti Malaya, 3rd Floor, Block A, 50603 Kuala Lumpur, Malaysia

Correspondence should be addressed to Chin Wei Lai; cwlai@um.edu.my

Received 30 January 2014; Revised 21 February 2014; Accepted 21 February 2014; Published 26 March 2014

Academic Editor: Tian-Yi Ma

One-dimensional calcium oxide (CaO-) based titanium dioxide (TiO_2) nanotubes were successfully synthesized through a rapid electrochemical anodization and chemical wet impregnation techniques. In this study, calcium nitrate solution was used as a calcium source precursor. The reaction time and concentration of calcium source on the formation of CaO-TiO_2 nanotubes were investigated using field emission microscopy, energy dispersion X-ray spectroscopy, and X-ray diffraction. The adsorption capacity of CO_2 was determined by thermal gravimetric analyzer. A maximum of 4.45 mmol/g was achieved from the CaO-TiO_2 nanotubes (6.64 at% of Ca). The finding was attributed to the higher active surface area for CaO to adsorb more CO_2 gas and then formed $CaCO_3$ compound during cyclic carbonation-calcination reaction.

1. Introduction

Recently, solid CO_2 adsorbents are used as an alternative and potentially less-energy-intensive separation technology. These CO_2 adsorbents can be utilized from ambient temperature up to 973 K by yielding less waste during cycle. In addition, their waste can be disposed of without undue environmental precautions as compared to liquid adsorbent [1]. A variety of solid physical adsorbents have been considered for CO_2 capture including microporous and mesoporous materials (carbon-based sorbents, such as activated carbon and carbon molecular sieves, zeolites, and chemically modified mesoporous materials), metal oxides, and hydrotalcite-like compounds [2, 3]. These listed adsorbents usually can be classified into three types based on their sorption/desorption temperatures: (1) low temperature adsorbent: <473 K (carbon, zeolites, MOFs/ZIFs, alkali metal carbonates, and amine-based materials), (2) intermediate temperature adsorbent: 473–673 K (hydrotalcite-like compounds, HTLcs/layered double hydroxides, LDHs), and (3) high-temperature adsorbents: >673 K (calcium based and alkali ceramic). The summary of those adsorbents with their efficiency and operating parameters are shown in Table 1.

According to Table 1, CaO and alkali ceramics are promising candidates for CO_2 adsorption. Therefore, CaO-based adsorbent has gained great attention due to its great capability (11.6 mmol/g) as compared to other adsorbents in capturing CO_2 gases through cyclic carbonation-calcination reaction. In addition, CaO-based adsorbent has high reactivity with CO_2 gases, high capacity, and low material cost [4]. The carbonation temperature for CaO-based adsorbents is between 873 and 973 K and their regeneration temperature is normally above 1223 K. The reversible reaction between CaO and CO_2 is

$$\mathrm{CaO\,(s) + CO_2\,(g) \rightleftharpoons CaCO_3\,(s)}$$
$$\Delta H^{\circ}_{873.15\,\mathrm{K}} = -171.2\,\mathrm{kJ\ mol^{-1}}\ \text{(for carbonation)} \quad (1)$$

In this manner, nanocrystalline of CaO has been proven to be useful in the noncatalytic removal of CO_2 in H_2 production [5]. The nanocrystalline of CaO with vacancies/defects, which often related to the presence of basic and acidic sites within their lattice. The structural defects normally are involved in the basic-acidic catalytic reactions. It is a well-known fact that CaO has highly reactive and strong basic sites because of the isolated O^{2-} centers as well as weak

Table 1: The different types of solid CO_2 adsorbents based on their sorption/desorption temperatures.

Adsorbent	Total capacity (mmol/g)	Temperature (K)	Pressure (atm)	Reference
Low temperature adsorbents				
Amine based				
Amine-modified mesoporous silica	4.5	348	1	(Liu et al., 2010) [12]
Amine-modified ordered mesoporous silica (OMS)	1.5	—	—	(Zeleňák et al., 2008) [13]
Amine-modified OMSs	0.2–1.4	348	1	(Liu et al., 2010) [12]
Amine tetraethylenepentamine (TEPA)/OMSs	4.6	348	1	(Liu et al., 2010) [12]
MOFs/ZIFs				
MOF-2	3.2	—	41	(Millward and Yaghi, 2005) [14]
Carbon/activated carbon based				
Coal-based activated carbon	0.3	323	0.001	(Deng et al., 2011) [15]
Porous carbon nitride (CN)	2.90	298	—	(Li et al., 2010) [16]
N-doped carbons template from zeolite	6.9	273	1	(Xia et al., 2011) [17]
Activated carbon/N_2	3.75			
Activated carbon/H_2	3.49	293	1	(Zhang et al., 2010) [18]
Activated carbon/NH_3	3.22			
Activated carbon	1.5	303	40	(Drage et al., 2009) [19]
Activated carbon	3.5	275	1	(Wang et al., 2008) [20]
Carbon nanotubes (CNTs)/3-aminopropyltriethoxysilane (APTS)	2.45	323	—	(Su et al., 2011) [21]
Alumina based				
γ-Al_2O_3	0.31	295	—	(Rege and Yang, 2001) [22]
Zeolite based				
Y-type zeolite/tetraethyl-enepentamine (TEPA)	4.27	303–333		(Su et al., 2010) [23]
Natural zeolite	2.05			
Treated zeolite/H_3PO_4	1.95	298	0.1	(Ertan and Çakicioğlu-Özkan, 2005) [24]
Synthetic zeolite-5X	5.49			
Synthetic zeolite-13A	6.82			
LilSX	0.17			
NaLX	0.23	—	1	(Brandani and Ruthven, 2004) [25]
CaX	0.24			
13X (NaX)	2.94	295	—	(Rege and Yang, 2001) [22]
Magnesium based				
MgO/Al_2O_3	1.36	333	1	(Li et al., 2010) [26]
Intermediate temperature adsorbents				
LDH				
Mg-Al-CO_3 LDHs	0.49	473	0.05	(Ram Reddy et al., 2006), [27]
High temperature adsorbents				
Lithium orthosilicates				
Li_4SiO_4	6.14	773	1	(Kato et al., 2002), [28]
Lithium zirconates				
Li_2ZrO_3	4.55	773	1	(Ida and Lin, 2003), [29]
Li_2ZrO_3	4.50	823	1	(Ochoa-Fernández et al., 2005), [30]
Li_2ZrO_3 (nanocrystalline)	6.14	848	1	(Ochoa-Fernández et al., 2006), [31]

Table 1: Continued.

Adsorbent	Total capacity (mmol/g)	Temperature (K)	Pressure (atm)	Reference
Calcium oxide based				
CaO	2.3	923	—	(Satrio et al., 2005), [32]
CaO/Al_2O_3	11.6	923	—	(Li et al., 2006), [33]
Cs/CaO	4.9	723	0.4	(Reddy and Smirniotis, 2004), [34]
Rb/CaO	4.5			
K/CaO	3.8			
Na/CaO	3.1			
$CaCO_3$	1.5	573	1	(Kuramoto et al., 2003), [35]
CaO/Al_2O_3	6.02	923	1	(Wu et al., 2007), [36]
Nano CaO/Al_2O_3	6.02	650	—	(Wu et al., 2008), [37]

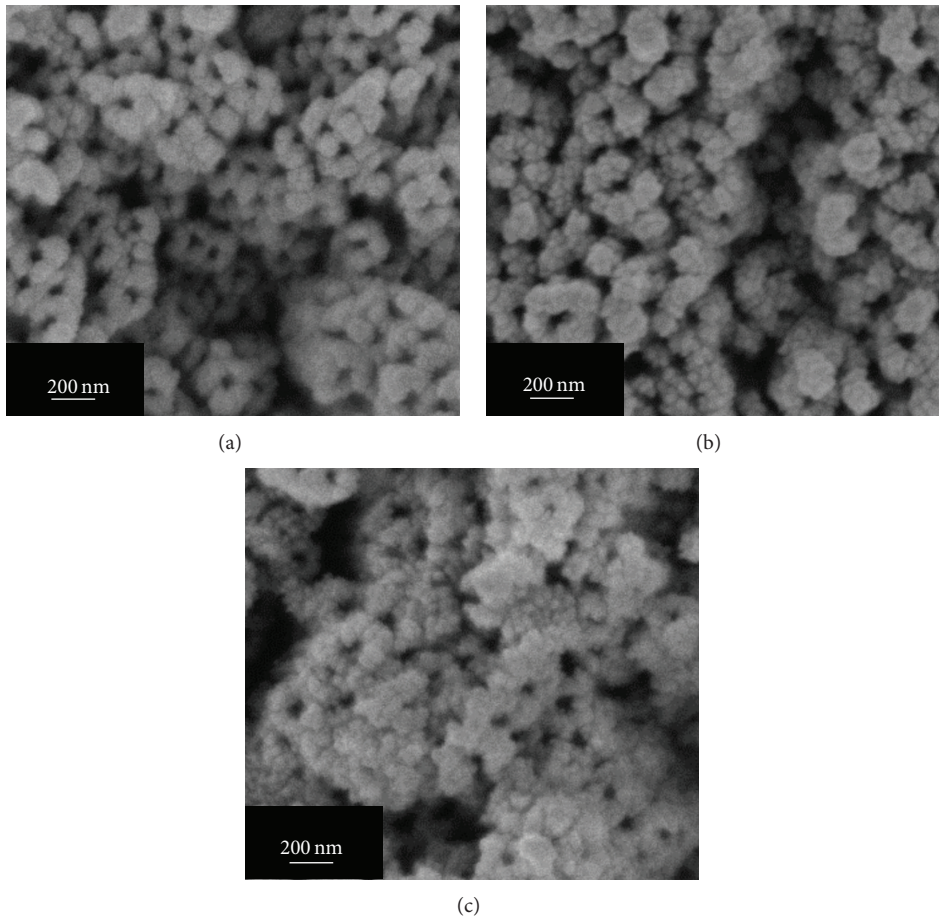

(a) (b) (c)

Figure 1: FESEM top view image of nanotubes subjected to wet impregnation of 0.6 M calcium nitrate solution for (a) 24 hours, (b) 48 hours, and (c) 72 hours and subsequent annealing at 673 K in Ar gas for 4 hours.

residual OH groups which appear when mixed with the rare earths [6]. However, these CO_2 adsorbents suffer severely from textural degradation during the sorption/desorption operations. These CO_2 adsorbents can only run several tens of cycles before any obvious degradation and are still far from practical applications [3]. Instantly, the conversion of CaO decreased sharply from 70% in the first cycle to 20% in the eleventh cycle when tested in fluidized bed [7]. The deactivation primarily results from the formation of thick layer structured from $CaCO_3$ surrounding the CaO, which severely hinders the diffusion of CO_2 gas to react with the inner core. Besides, it has also been reported that the adsorption capacity for CaO-based sorbents decays as a function of the sintering of CaO grain at high temperature

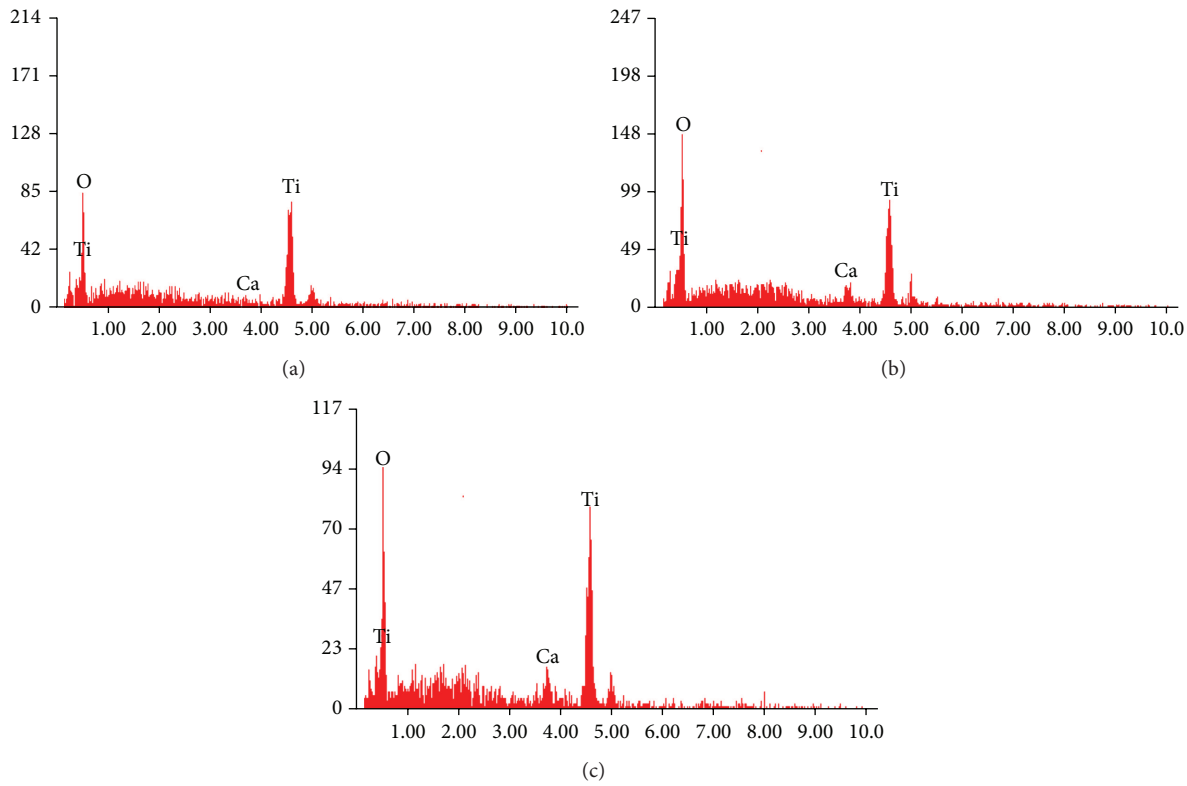

FIGURE 2: EDX spectra of nanotubes subjected to wet impregnation of 0.6 M calcium nitrate solution for (a) 24 hours, (b) 48 hours, and (c) 72 hours (all EDX spectrums are noneditable format based on our FESEM-EDX system).

and a certain loss in the porosity. When pores smaller than a critical value (e.g., 200 nm) are filled, the reaction gets much slower [8]. Therefore, great efforts have to be made in order to further improve the cyclic stability of CaO-based sorbents.

One of the most promising solutions to improve the cyclic stability of CaO is controlling their architecture into one-dimensional nanomaterials. The main reason might be attributed to the fast reaction (chemical reaction) and the slow reaction (diffusion controlled) could be achieved during CO_2 adsorption. In this case, the diffusion of CO_2 into the particle interior to react with Ca dopants could be prevented and the whole CO_2 adsorption process could then be diffusion-controlled [2, 3]. Theoretically, the small particles size of sorbent (e.g., 30–50 nm) would perform better carbonation-calcination reaction, which allowed carbonation to take place at the rapid reaction-controlled regime. Another promising solution to improve cyclic stability is to incorporate high stability metal oxide (titanium dioxide) into CaO particles. The prevention of CaO oxidation during calcination stage could be expected. Therefore, detail investigation on one-dimensional CaO-TiO_2 nanotubes for effective CO_2 adsorption will be discussed.

2. Experimental Procedure

One-dimensional TiO_2 nanotube arrays were synthesized using a rapid-anodic oxidation electrochemical anodization technique. A high purity of Ti foil (99.6%, Strem Chemical, USA) with a thickness of 127 μm was selected as substrate to grow TiO_2 nanotubes. This process was conducted in a bath with electrolytes composed of ethylene glycol ($C_2H_6O_2$, >99.5%, Merck, USA), 5 wt% ammonium fluoride (NH_4F, 98%, Merck, USA), and 5 wt% hydrogen peroxide (H_2O_2, 30% H_2O_2 and 70% H_2O, J. T. Baker, USA) for 60 minutes at 60 V. This experimental condition was selected because it favors the formation of well-aligned TiO_2 nanotube arrays [9, 10]. After the anodization process, as-anodized samples were cleaned using distilled water and dried under a nitrogen stream. CaO-TiO_2 nanotubes were then prepared through wet impregnation technique using calcium nitrate tetrahydrate ($Ca(NO_3)_2{\cdot}4H_2O$, Merck, USA) as the precursor. This was an ex situ approach that was used to incorporate Ca^{2+} ions into TiO_2 nanotubes. Two different concentrations of calcium nitrate tetrahydrate solution (0.6, 1.2 M) were prepared at different reaction times (24, 48, 72 hours) in a water bath of 80°C. Subsequently, the samples were thermal-annealed at 673 K in an argon atmosphere for 4 h in order to produce crystalline TiO_2 nanotubes.

The surface morphologies of the synthesized samples were observed through field emission scanning electron microscopy (FESEM) using a Zeiss SUPRA 35 VP, which is operated at a working distance of 1 mm and 5 kV. The energy dispersive X-ray spectroscopy (EDX) was applied to elemental analysis of the CaO-TiO_2 nanotubes sorbents, which is equipped in the FESEM. The structural variations and phase determination for CaO-TiO_2 nanotubes sorbents

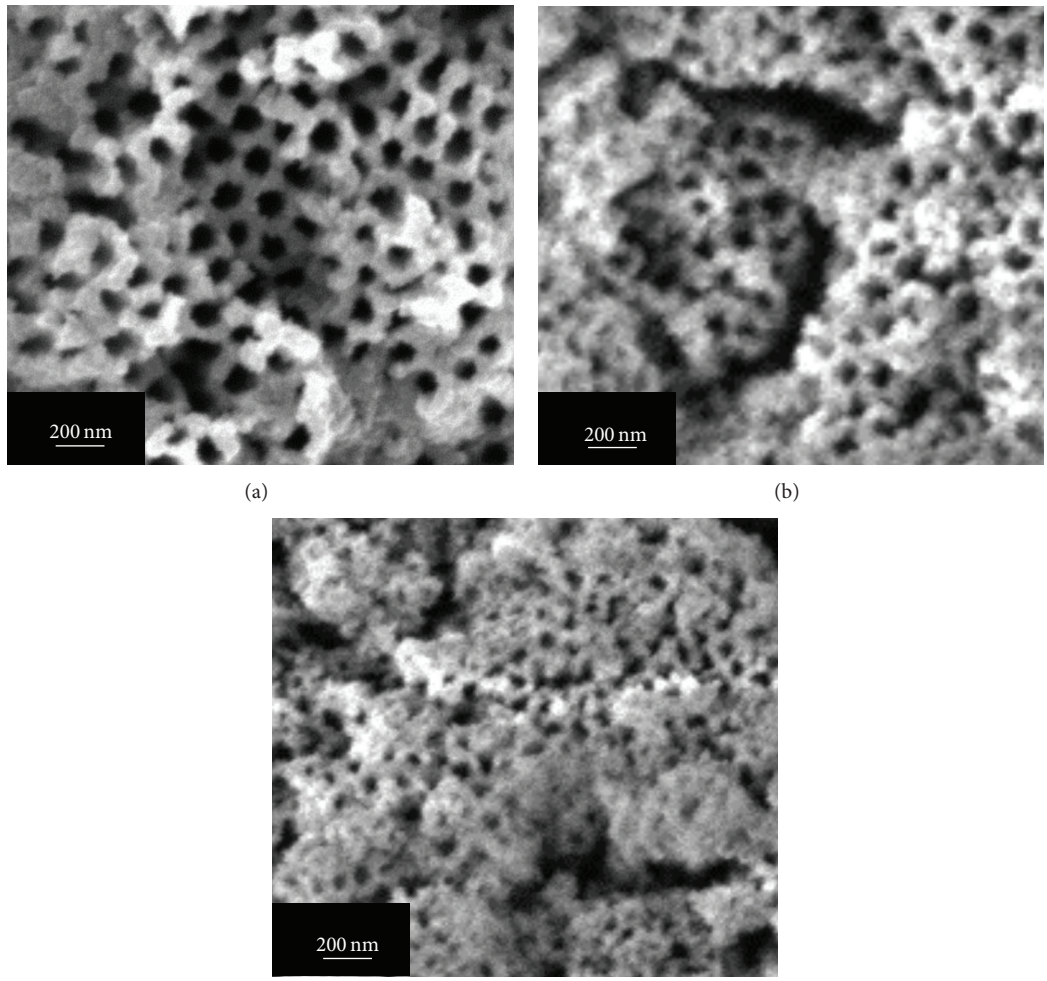

(a) (b) (c)

Figure 3: FESEM top view image of nanotubes subjected to wet impregnation of 1.2 M calcium nitrate solution for (a) 24 hours, (b) 48 hours, and (c) 72 hours and subsequent annealing at 673 K in Ar gas for 4 hours.

were determined using a Philips PW 1729 X-ray diffraction (XRD), which operated at 45 kV and 40 mV patterns. The thermogravimetric analysis (TGA) was used to investigate the CO_2 adsorption for CaO-TiO_2 nanotubes sorbents (STA 6000, Perkin Elmer, USA). The steps included are N_2 gas flow at a rate of 10°C/min from room temperature to 673 K and then holding for 30 min in CO_2 and finally cooling down to 573 K by N_2 gas. In the present study, carbonation-calcination reaction is set to be 673 K because nanotubular structure can be collapsed at high temperature (above 773 K) [11].

3. Results and Discussion

The surface morphologies of CaO-TiO_2 nanotubes synthesized in 0.6 M calcium nitrate solution for 24, 48, and 72 hours were subsequently observed via FESEM as presented in Figures 1(a) to 1(c), respectively. As shown in the FESEM images, the opening of the nanotubular structure showed aggregation of CaO species on wall surface of TiO_2 nanotubes. The wall thickness of the nanotubes dramatically increased to 75 nm, which resulted in a narrow pore entrance for 24 hours reaction time (Figure 1(a)). Meanwhile, as the reaction time increased to 48 hours, the wall thickness of the nanotubes increased from about 75 nm to 100 nm (Figure 1(b)). With further increase of the reaction time to 72 hours, it was found that the nanotubes were covered with excess CaO species and clogged the pore entrance (Figure 1(c)). A rough, irregular, and corrugated surface was formed. Based on the FESEM images, it could be concluded that the appearance of TiO_2 nanotubes was dependent on the reaction time in calcium nitrate solution. A narrow or blocked pore entrance of nanotubes was formed as increasing soaking period in the solution. Next, the average atomic percentage (at%) of the elements within CaO-TiO_2 nanotubes was determined using EDX analysis. The numerical EDX analyses of the samples are listed in Table 2. As determined through EDX analysis, the average Ca contents of the nanotubes for 24, 48, and 72 hours were 1.01 at%, 3.67 at%, and 4.59 at%, respectively. The intensity of the Ca peak (3.69 keV) increased with increasing reaction time in calcium nitrate solution as presented in

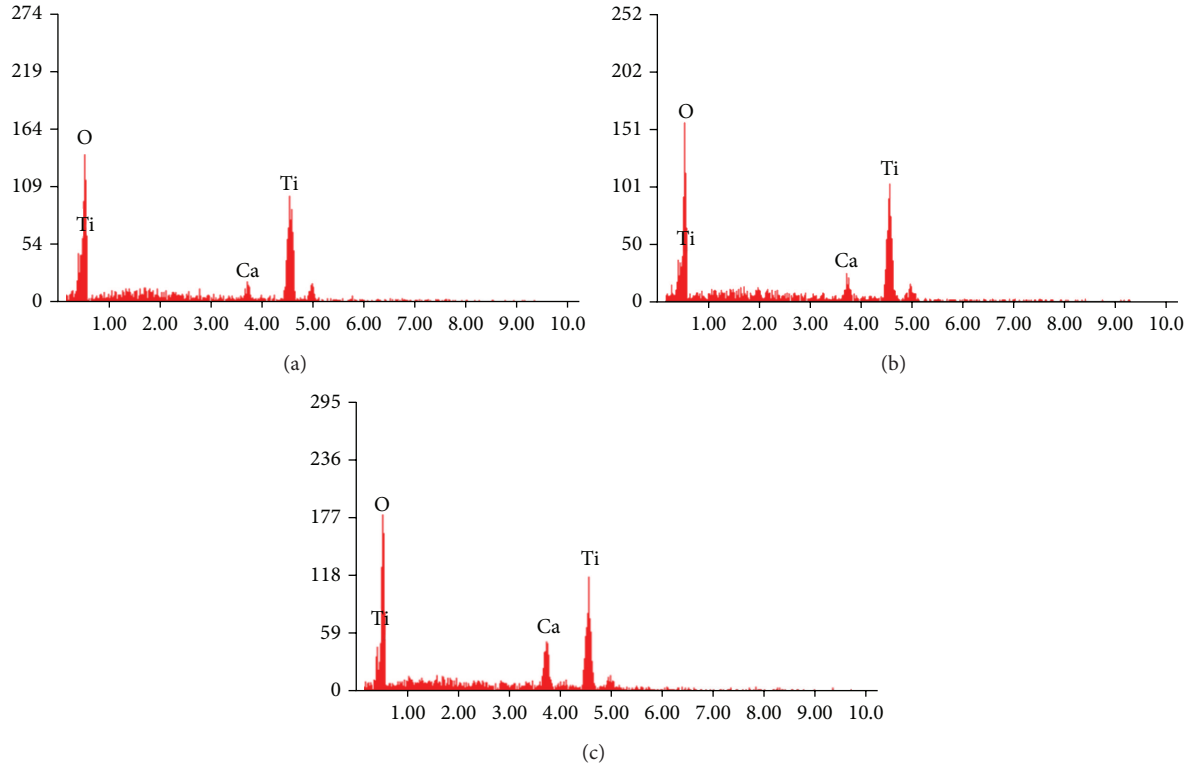

Figure 4: EDX spectra of nanotubes subjected to wet impregnation of 1.2 M calcium nitrate solution for (a) 24 hours, (b) 48 hours, and (c) 72 hours (all EDX spectrums are noneditable format based on our FESEM-EDX system).

Figures 2(a) to 2(c). Another set of experiments was conducted to form CaO-TiO_2 nanotubes in 1.2 M calcium nitrate solution for 24, 48, and 72 hours. All morphologies of the samples showed similar appearance of CaO-TiO_2 nanotubes synthesized in 0.6 M calcium nitrate solution. The irregular CaO layer covered all of the TiO_2 nanotubular structure and nanoporous structure arranged in a nonordered manner which could be observed in Figures 3(a) to 3(c). The chemical stoichiometry of the resultant samples was determined via EDX analysis as shown in Figures 4(a) to 4(c). A high Ca content of 9.78 at% was determined from those synthesized in 1.2 M calcium nitrate solution for 72 hours, indicating that the incorporation of the CaO became prominent with increasing the concentration of calcium nitrate solution. Based on the FESEM images and EDX analysis, the small Ca^{2+} ions could be diffused into TiO_2 nanotubes in the presence of lattice defects, especially nearby to the wall of nanotubes. In this case, the diffusion rate of Ca^{2+} ions increased significantly when increasing the reaction time and concentration of precursor. However, the content of small Ca^{2+} ions that diffused into the TiO_2 lattice could reach a saturation condition and start to accumulate on the surface of nanotubes. The number of nucleation sites for Ca^{2+} ions loaded on the wall surface of the nanotubes increased with longer reaction time and higher concentration of precursor, which produced nanotubes with thicker walls. The diffusion of the Ca^{2+} ions formed Ca–O bonding with O–Ti–O bonding; thus, charge neutrality could be achieved.

Table 2: EDX result of CaO-TiO_2 with different soaking time in 0.6 M and 1.2 M calcium nitrate solution.

Concentration of calcium nitrate solution (M)	Element (at%)/reaction time (h)	Ti	O	Ca
0.6	24	46.07	52.92	01.01
	48	38.88	57.45	03.67
	72	42.30	53.11	04.59
1.2	24	36.44	60.66	02.90
	48	32.64	60.64	06.64
	72	28.83	61.10	09.78

In the present study, XRD analysis was used to determine the crystallographic structure and the changes in the phase structure of the CaO-TiO_2 nanotubes synthesized in different reaction times and concentrations of precursor are presented in Figures 5 and 6. Numerous studies reported that heat treatment at about 400°C could transform the amorphous structure of TiO_2 into the crystalline anatase phase. The obvious diffraction peaks from the XRD pattern attributed to the anatase phase (JCPDS no. 21-1272) were detected from the XRD patterns (Figure 5(a)). The diffraction peaks are allocated at 25.32°, 37.84°, 38.42°, 48.02°, 53.87°, 55.09°, 62.93°, 70.65°, and 76.23°, which correspond to 101, 004, 112, 200, 105, 211, 204, 220, and 301 crystal planes for the anatase

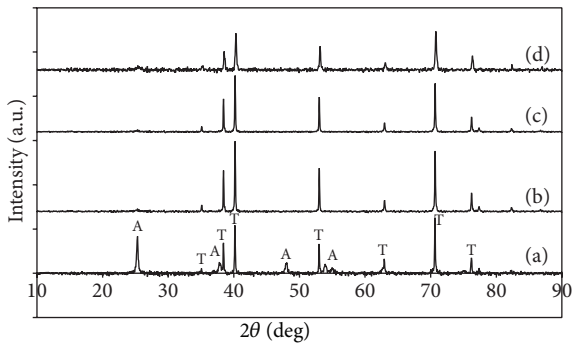

Figure 5: XRD pattern of TiO_2 nanotubes incorporated with Ca in 0.6 M $Ca(NO_3)_2$ solution at different soaking period: (a) pure TiO_2, (b) 24 hours, (c) 48 hours, and (d) 72 hours (A = anatase phase; T = titanium phase).

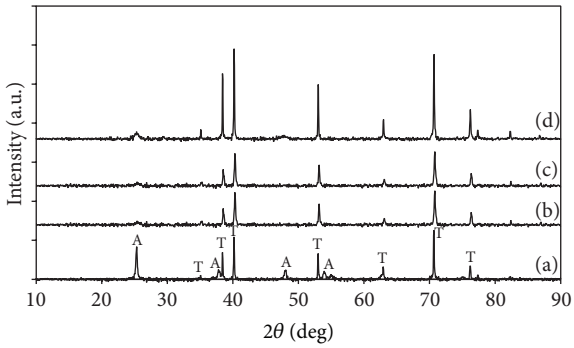

Figure 6: XRD pattern of TiO_2 nanotubes incorporated with Ca in 1.2 M $Ca(NO_3)_2$ solution at different soaking period: (a) pure TiO_2, (b) 24 hours, (c) 48 hours, and (d) 72 hours (A = anatase phase; T = titanium phase).

phase, respectively. Apparently, the incorporation of Ca^{2+} ions into the lattice of TiO_2 hindered the crystallization of TiO_2, resulting in the peak intensity of the 101 peak at 25.32° decrease. The decrease in anatase phase is maybe due to the interruption of Ca atom, which diffused into TiO_2 nanotubes and inhibited the formation of the anatase. The XRD pattern of the sample soaked in 1.2 M for 72 hours exhibits additional peaks 220 and 400 crystal planes at 54° and 80°, corresponding to CaO phase. This indicates that crystalline CaO are formed once the concentration of Ca in TiO_2 reaches a higher level. Next, the resultant anodized CaO-TiO_2 nanotubes were used in the characterization of CO_2 adsorption using TGA analysis. The processing steps involved in TGA analysis are N_2 gas flow at a rate of 10°C/min from room temperature to 673 K and then holding for 30 min in CO_2 and finally cooling down to 573 K by N_2 gas. The TGA curves for 0.6 M of Ca and 1.2 M of Ca are shown in Figures 7 and 8, respectively, while the CO_2 adsorption capacity is summarized in Table 3. Based on the TGA analysis, it could be observed that all CaO-TiO_2 samples showed their CO_2 adsorption capacity in the range of 3.3 mmol/g to 4.5 mmol/g. A maximum CO_2 adsorption capacity of up to 4.45 mmol/g was observed from the CaO-TiO_2 nanotubes synthesized in

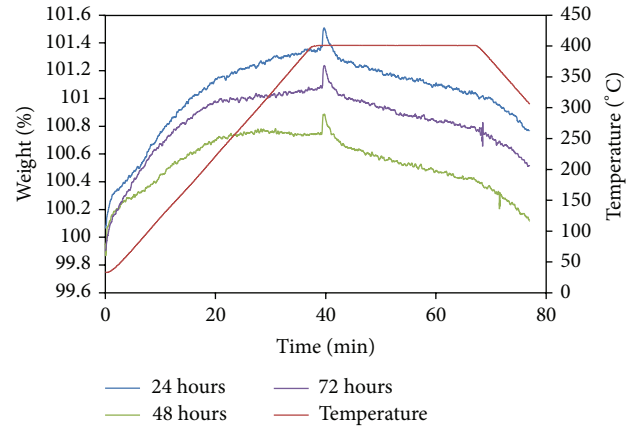

Figure 7: TGA curve of soaking in 0.6 M of Ca for different periods of time.

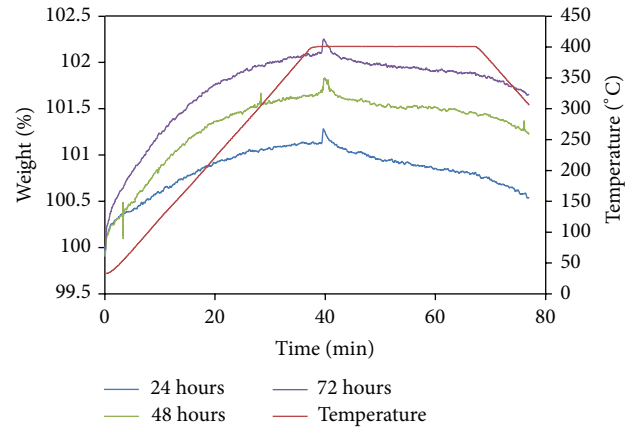

Figure 8: TGA curve of soaking in 1.2 M of Ca for different periods of time.

Table 3: CO_2 adsorption capacity of the CaO-TiO_2 samples.

Concentration of calcium nitrate solution (M)	Soaking period (hours)	CO_2 adsorption capacity (mmol/g)
0.6	24	3.89
	48	3.32
	72	4.00
1.2	24	3.59
	48	4.45
	72	3.80

1.2 M of calcium nitrate solution for 48 hours. Basically, the CO_2 adsorption capacity based CaO-TiO_2 sorbents used the following reaction: $CaO + CO_2 \rightarrow CaCO_3$. In this case, the sorbent weight is increased significantly when CO_2 gas is applied to the TGA system, where all the weight added is CO_2 adsorbed. This reason clearly explains that CO_2 adsorption capacity is increased after carbonation process.

4. Conclusion

The present study demonstrated that one-dimensional CaO-TiO_2 nanotubes sorbent was successfully formed using oxidation electrochemical anodization and wet impregnation techniques. All of the resultant CaO-TiO_2 nanotubes sorbent exhibited promising CO_2 adsorption capacity in the range of 3.3 mmol/g to 4.5 mmol/g. It is shown that high active surface area of CaO-TiO_2 nanotubes sorbent showed good stability during extended cyclic carbonation-calcination reaction.

Conflict of Interests

The author declares that there is no conflict of interests regarding the publication of this paper.

Acknowledgments

This research is supported by High Impact Research Chancellory Grant UM.C/625/1/HIR/228 (J55001-73873) from the University of Malaya. In addition, authors would like to thank University of Malaya for sponsoring this work under University of Malaya Research Grant (UMRG, no. RP022-2012D).

References

[1] Q. Wang, J. Luo, Z. Zhong, and A. Borgna, "CO_2 capture by solid adsorbents and their applications: current status and new trends," *Energy & Environmental Science*, vol. 4, no. 1, pp. 42–55, 2011.

[2] D. M. D'Alessandro, B. Smit, and J. R. Long, "Carbon dioxide capture: prospects for new materials," *Angewandte Chemie International Edition*, vol. 49, no. 35, pp. 6058–6082, 2010.

[3] S. Wang, S. Yan, X. Ma, and J. Gong, "Recent advances in capture of carbon dioxide using alkali-metal-based oxides," *Energy & Environmental Science*, vol. 4, no. 10, pp. 3805–3819, 2011.

[4] N. H. Florin and A. T. Harris, "Reactivity of CaO derived from nano-sized $CaCO_3$ particles through multiple CO_2 capture-and-release cycles," *Chemical Engineering Science*, vol. 64, no. 2, pp. 187–191, 2009.

[5] J. García, T. López, M. Álvarez, D. H. Aguilar, and P. Quintana, "Spectroscopic, structural and textural properties of CaO and CaO-SiO_2 materials synthesized by sol-gel with different acid catalysts," *Journal of Non-Crystalline Solids*, vol. 354, no. 2-9, pp. 729–732, 2008.

[6] V. R. Choudhary, S. A. R. Mulla, and B. S. Uphade, "Oxidative coupling of methane over alkaline earth oxides deposited on commercial support precoated with rare earth oxides," *Fuel*, vol. 78, no. 4, pp. 427–437, 1999.

[7] D. Alvarez and J. C. Abanades, "Pore-size and shape effects on the recarbonation performance of calcium oxide submitted to repeated calcination/recarbonation cycles," *Energy and Fuels*, vol. 19, no. 1, pp. 270–278, 2005.

[8] J.-R. Li, Y. Ma, M. C. McCarthy et al., "Carbon dioxide capture-related gas adsorption and separation in metal-organic frameworks," *Coordination Chemistry Reviews*, vol. 255, no. 15-16, pp. 1791–1823, 2011.

[9] S. Sreekantan, L. C. Wei, and Z. Lockman, "Extremely fast growth rate of TiO_2 nanotube arrays in electrochemical bath containing H_2O_2," *Journal of the Electrochemical Society*, vol. 158, no. 12, pp. C397–C402, 2011.

[10] C. W. Lai and S. Sreekantan, "Dimensional control of TiO_2 nanotube arrays with H_2O_2 content for high photoelectrochemical water splitting performance," *Micro & Nano Letters*, vol. 7, no. 5, pp. 443–447, 2012.

[11] Y. K. Lai, J. Y. Huang, H. F. Zhang et al., "Nitrogen-doped TiO_2 nanotube array films with enhanced photocatalytic activity under various light sources," *Journal of Hazardous Materials*, vol. 184, no. 1–3, pp. 855–863, 2010.

[12] S.-H. Liu, C.-H. Wu, H.-K. Lee, and S.-B. Liu, "Highly stable amine-modified mesoporous silica materials for efficient CO_2 capture," *Topics in Catalysis*, vol. 53, no. 3-4, pp. 210–217, 2010.

[13] V. Zeleňák, M. Badaničová, D. Halamová et al., "Amine-modified ordered mesoporous silica: effect of pore size on carbon dioxide capture," *Chemical Engineering Journal*, vol. 144, no. 2, pp. 336–342, 2008.

[14] A. R. Millward and O. M. Yaghi, "Metal-organic frameworks with exceptionally high capacity for storage of carbon dioxide at room temperature," *Journal of the American Chemical Society*, vol. 127, no. 51, pp. 17998–17999, 2005.

[15] H. Deng, H. Yi, X. Tang, P. Ning, and Q. Yu, "Adsorption of CO_2 and N_2 on coal-based activated carbon," *Advanced Materials Research*, vol. 204-210, pp. 1250–1253, 2011.

[16] Q. Li, J. Yang, D. Feng et al., "Facile synthesis of porous carbon nitride spheres with hierarchical three-dimensional mesostructures for CO_2 capture," *Nano Research*, vol. 3, no. 9, pp. 632–642, 2010.

[17] Y. Xia, R. Mokaya, G. S. Walker, and Y. Zhu, "Superior CO_2 adsorption capacity on N-doped, high-surface-area, microporous carbons templated from zeolite," *Advanced Energy Materials*, vol. 1, pp. 678–683, 2011.

[18] Z. Zhang, M. Xu, H. Wang, and Z. Li, "Enhancement of CO_2 adsorption on high surface area activated carbon modified by N_2, H_2 and ammonia," *Chemical Engineering Journal*, vol. 160, no. 2, pp. 571–577, 2010.

[19] T. C. Drage, J. M. Blackman, C. Pevida, and C. E. Snape, "Evaluation of activated carbon adsorbents for CO_2 capture in gasification," *Energy and Fuels*, vol. 23, no. 5, pp. 2790–2796, 2009.

[20] Y. Wang, Y. Zhou, C. Liu, and L. Zhou, "Comparative studies of CO_2 and CH_2 sorption on activated carbon in presence of water," *Colloids and Surfaces A: Physicochemical and Engineering Aspects*, vol. 322, no. 1–3, pp. 14–18, 2008.

[21] F. Su, C. Lu, and H.-S. Chen, "Adsorption, desorption, and thermodynamic studies of CO_2 with high-amine-loaded multiwalled carbon nanotubes," *Langmuir*, vol. 27, no. 13, pp. 8090–8098, 2011.

[22] S. U. Rege and R. T. Yang, "A novel FTIR method for studying mixed gas adsorption at low concentrations: H_2O and CO_2 on NaX zeolite and γ-alumina," *Chemical Engineering Science*, vol. 56, no. 12, pp. 3781–3796, 2001.

[23] F. Su, C. Lu, S.-C. Kuo, and W. Zeng, "Adsorption of CO_2 on amine-functionalized y-type zeolites," *Energy and Fuels*, vol. 24, no. 2, pp. 1441–1448, 2010.

[24] A. Ertan and F. Çakicioğlu-Özkan, "CO_2 and N_2 adsorption on the acid (HCl, HNO_3, H_2SO_4 and H_3PO_4) treated zeolites," *Adsorption*, vol. 11, no. 1, pp. 151–156, 2005.

[25] F. Brandani and D. M. Ruthven, "The effect of water on the adsorption of CO_2 and C_3H_8 on type X zeolites," *Industrial & Engineering Chemistry Research*, vol. 43, no. 26, pp. 8339–8344, 2004.

[26] L. Li, X. Wen, X. Fu et al., "MgO/Al_2O_3 sorbent for CO_2 capture," *Energy and Fuels*, vol. 24, no. 10, pp. 5773–5780, 2010.

[27] M. K. Ram Reddy, Z. P. Xu, G. Q. Lu, and J. C. D. Da Costa, "Layered double hydroxides for CO_2 capture: structure evolution and regeneration," *Industrial & Engineering Chemistry Research*, vol. 45, no. 22, pp. 7504–7509, 2006.

[28] M. Kato, S. Yoshikawa, and K. Nakagawa, "Carbon dioxide absorption by lithium orthosilicate in a wide range of temperature and carbon dioxide concentrations," *Journal of Materials Science Letters*, vol. 21, no. 6, pp. 485–487, 2002.

[29] J.-I. Ida and Y. S. Lin, "Mechanism of high-temperature CO_2 sorption on lithium zirconate," *Environmental Science and Technology*, vol. 37, no. 9, pp. 1999–2004, 2003.

[30] E. Ochoa-Fernández, H. K. Rusten, H. A. Jakobsen, M. Rønning, A. Holmen, and D. Chen, "Sorption enhanced hydrogen production by steam methane reforming using Li_2ZrO_3 as sorbent: sorption kinetics and reactor simulation," *Catalysis Today*, vol. 106, no. 1-4, pp. 41–46, 2005.

[31] E. Ochoa-Fernández, M. Rønning, T. Grande, and D. Chen, "Synthesis and CO_2 capture properties of nanocrystalline lithium zirconate," *Chemistry of Materials*, vol. 18, no. 25, pp. 6037–6046, 2006.

[32] J. A. Satrio, B. H. Shanks, and T. D. Wheelock, "Development of a novel combined catalyst and sorbent for hydrocarbon reforming," *Industrial & Engineering Chemistry Research*, vol. 44, no. 11, pp. 3901–3911, 2005.

[33] Z.-S. Li, N.-S. Cai, and Y.-Y. Huang, "Effect of preparation temperature on cyclic CO_2 capture and multiple carbonation-calcination cycles for a new Ca-based CO_2 sorbent," *Industrial & Engineering Chemistry Research*, vol. 45, no. 6, pp. 1911–1917, 2006.

[34] E. P. Reddy and P. G. Smirniotis, "High-temperature sorbents for CO_2 made of alkali metals doped on CaO supports," *The Journal of Physical Chemistry B*, vol. 108, no. 23, pp. 7794–7800, 2004.

[35] K. Kuramoto, S. Fujimoto, A. Morita et al., "Repetitive carbonation-calcination reactions of Ca-based sorbents for efficient CO_2 sorption at elevated temperatures and pressures," *Industrial & Engineering Chemistry Research*, vol. 42, no. 5, pp. 975–981, 2003.

[36] S. F. Wu, T. H. Beum, J. I. Yang, and J. N. Kim, "Properties of Ca-base CO_2 sorbent using $Ca(OH)_2$ as precursor," *Industrial & Engineering Chemistry Research*, vol. 46, no. 24, pp. 7896–7899, 2007.

[37] S. F. Wu, Q. H. Li, J. N. Kim, and K. B. Yi, "Properties of a nano CaO/Al_2O_3 CO_2 sorbent," *Industrial & Engineering Chemistry Research*, vol. 47, no. 1, pp. 180–184, 2008.